Polyhedral Oligomeric Silsesquioxane–Polyphenylsulfone Nanocomposites: Investigation of the Melt-Flow Enhancement, Thermal Behavior, and Mechanical Properties

Paul J. Jones,[1] Robert D. Cook,[1] Cynthia N. McWright,[1] Raymond J. Nalty,[1] Veena Choudhary,[2] Sarah E. Morgan[1]

[1]*School of Polymers and High Performance Materials, University of Southern Mississippi, Polymer Science Building, Room 303, 118 College Drive #5050, Hattiesburg, Mississippi 39406-0001*
[2]*India Centre for Polymer Science & Engineering, Indian Institute of Technology, New Delhi, Hauz Khas, New Delhi 110 016, India*

Received 14 April 2010; accepted 25 November 2010
DOI 10.1002/app.33852
Published online 30 March 2011 in Wiley Online Library (wileyonlinelibrary.com).

ABSTRACT: Two structurally and chemically different polyhedral oligomeric silsesquioxane (POSS) molecules with different solubility parameters, dodecaphenyl POSS and trisilanolphenyl POSS, were melt-blended with polyphenylsulfone (PPSU), and the effects on the material processing, rheology, and thermomechanical properties were investigated. Process monitoring and capillary rheometry revealed enhancements in the processing melt flow and a reduction in the nanocomposite viscosity with only a small addition of POSS. The magnitude and concentration dependence of rheological modification were shown to depend on POSS structure. Although small increases in the tensile modulus were observed, reductions in the tensile elongation properties were observed at high POSS loading levels. Analysis of the nanocomposite fracture behavior and surface morphology provided evidence for the surface phase segregation of both types of POSS, but the extent of segregation was related to the POSS structure. The degree of interfacial adhesion in the POSS/polymer composites and the resultant rheological behavior were related to the POSS composition and predicted solubility parameters. No measurable effect on the glass-transition temperature or molecular weight of PPSU was observed, whereas small improvements in the thermal degradation behavior were obtained with the incorporation of POSS. © 2011 Wiley Periodicals, Inc. J Appl Polym Sci 121: 2945–2956, 2011

Key words: Nanocomposites; rheology; high performance polymers; POSS; thermoplastics

INTRODUCTION

Polyhedral oligomeric silsesquioxanes (POSSs) are a unique class of nanoparticles with a hybrid organic–inorganic structure, well-defined three-dimensional architecture, and monodisperse particle size. They are the subject of intense scientific and commercial interest because of their potential to provide enhanced properties when they are incorporated into a polymer matrix. POSS molecules consist of an Si—O—Si inorganic cage surrounded by an organic corona, represented by R substituents. The inorganic cage, with the structure $(SiO_{1.5})_n$, where $n = 8$, 10, or 12, may be a fully condensed closed cage or an open silanol structure.[1,2] The diameter of the nanocages ranges from 1 to 3 nm, depending on the composition of the molecule.[3] The organic substituents can be tailored to provide a wide range of properties. They can also be modified to enhance the compatibility with a specific polymer matrix[4–6] or made reactive to allow copolymerization with a spectrum of monomers.

The incorporation of POSS molecules into a polymer matrix can proceed by copolymerization or physical blending methods. Although most studies have focused on the synthesis of POSS copolymers,[7–16] relatively few studies have been performed on melt-blended systems.[17–19] Investigations of melt-mixed systems have revealed a correlation between the nanocomposite rheological behavior and POSS composition and loading level. This behavior deviates from the classical theory for hard-sphere-filled suspensions, which predicts a monotonic increase in the viscosity with increasing particle loading.[20] Joshi et al.[21] performed an investigation into the rheological and viscoelastic properties of melt-mixed

Correspondence to: S. E. Morgan (sarah.morgan@usm.edu).

Contract grant sponsor: National Science Foundation; contract grant number: EEC-0602032.
Contract grant sponsor: Solvay Advanced Polymers.

high-density polyethylene/POSS composites. They report that low POSS concentrations (0.25–0.5 wt %) reduced the complex viscosity, whereas higher concentrations caused the complex viscosity to increase. This behavior was attributed to the limited solubility of POSS in high-density polyethylene at low concentrations, whereas above the solubility limit, POSS agglomeration occurred, and viscosity increased. Kopesky et al.[22] reported a minimum in the zero-shear viscosity at low POSS loadings (<5 vol %) in melt-mixed poly(methyl methacrylate) POSS blends. Two different types of flow regimes were proposed for melt-mixed POSS systems. In the low-concentration regime, POSS was molecularly dispersed, and the viscosity was reduced. In the higher concentration regime, after the solubility limit was reached, the crystallization and agglomeration of POSS occurred, and the system behaved as a hard-sphere-filled suspension. Zhou et al.[23] reported a minimum in the complex viscosity at a POSS concentration of 1 wt % for physically blended systems containing POSS and polypropylene. They suggested that Cole–Cole plots indicated fine dispersion at POSS concentrations below 1%, with POSS aggregation at concentrations higher than 1%. Studies of other types of nanoparticles (ca. $\leq$10 nm) have indicated that weak polymer–particle interactions cause the behavior of the system to deviate from the classical theory for hard-sphere-filled suspensions and result in a strong decrease in the viscosity at low concentrations followed by an increase in the viscosity at higher concentrations.[24,25] For the purpose of this article, this phenomenon is referred to as the nanoparticle effect.

Studies in our own and other research laboratories have demonstrated the propensity of POSS to segregate to the surface of a polymer matrix.[26–32] The POSS surface-enriched nanocomposites exhibit reduced friction and melt viscosity and improved surface hardness, abrasion resistance, and hydrophobicity. The level of property improvement is related to the extent of segregation and POSS molecular aggregation, which is, in turn, related to the POSS concentration and solubility in the polymer matrix. The surface segregation behavior may be related to the rheology enhancement observed in POSS composites. It has also been suggested that the melting temperatures and relative viscosities of the polymer and POSS molecules may play a role in rheology modification.[33] However, these factors do not fully explain the observed rheological behavior, and the mechanism is not well understood.

Solubility parameters are often used to predict compatibility.[34] A minimum in the enthalpy of mixing (ΔH_m) is predicted when the difference in the solubility parameters is minimized by the following relation:[35]

$$\Delta H_m = V(\delta_1 - \delta_2)^2 \phi_1 \phi_2 \quad (1)$$

where V is the volume of the system, ϕ is the volume fraction, δ is the solubility parameter, and the subscripts 1 and 2 refer to components of the mixture. If the difference in solubility parameters is close to zero, a low ΔH_m is predicted; this indicates potential compatibility.[36]

This study was conducted in an attempt to understand the relationship between POSS solubility in a thermoplastic polyphenylsulfone (PPSU) matrix and the resulting composite rheology and material processing. PPSU is a high-performance engineering thermoplastic with a high toughness, chemical resistance, and thermal stability. It was of interest to determine the effects of the POSS incorporation on the processing enhancement and mechanical properties of a PPSU matrix. PPSU and two different grades of POSS, a closed-cage dodecaphenyl polyhedral oligomeric silsesquioxane (Dp-POSS) and an open cage trisilanolphenyl dodecaphenyl (Tsp-POSS), were identified for evaluation for their possible compatibility with PPSU. The compatibility was predicted by the calculation of the solubility parameters with the method established by Hoy.[37] Material processing was investigated by analysis of the extruder torque during melt blending and the mold pressure during injection molding. The composite melt rheology was assessed with capillary rheometry. The molecular weights of PPSU and the POSS/PPSU nanocomposites were measured by gel permeation chromatography (GPC). The thermal behavior of the POSS/PPSU systems was examined with a combination of differential scanning calorimetry (DSC) and thermogravimetric analysis (TGA). Optical microscopy was used to investigate the composite morphology, and the tensile properties of the molded test specimens were evaluated to determine the effects of POSS incorporation on the mechanical performance.

EXPERIMENTAL

Materials

PPSU resin (trade name Radel R5100NT) was supplied by Solvay Advanced Polymers, LLC (Alpharetta, GA). This grade of PPSU has a reported modulus of 2.3 GPa and a tensile strength of 70 MPa. It is a ductile polymer with reported percentage elongation at yield of 7.2% and a percentage elongation at break that ranges from 60 to 120%[38] (see Fig. 1). Dp-POSS (MS0802) and Tsp-POSS (SO1458) were supplied as dry white powders by Hybrid Plastics, Inc. (Hattiesburg, MS).

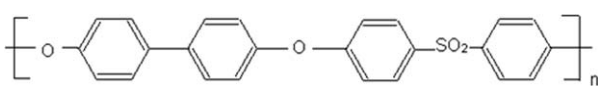

Figure 1 Chemical structure of PPSU.

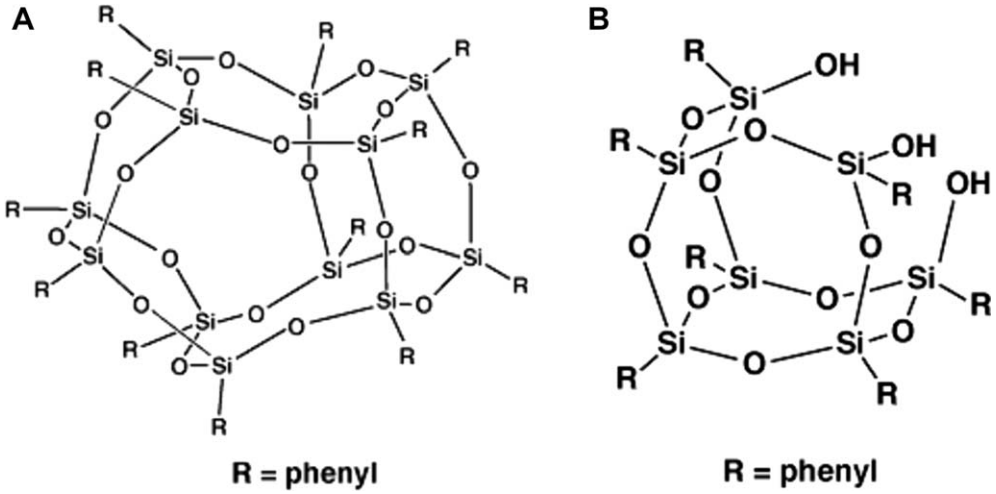

Figure 2 Chemical structures of the POSS chemicals: (A) Dp-POSS and (B) Tsp-POSS.

The molecular structures of the two grades of POSS are shown in Figure 2.

Composite blending and sample preparation

POSS/PPSU nanocomposites were prepared with a B&P Process CT 25 twin-screw extruder (screw diameter = 25 mm, length-to-diameter ratio = 40 : 1, three-hole die with a diameter of 3/16 in.) equipped with high-shear screws. The extrusion parameters were as follows: feed rate = 20 lb/h; screw speed = 950 rpm; and barrel temperatures = 205°C in the feed section, 270–355°C in the compression zone, 355°C in the metering section, and 316°C in the die. The melt temperatures were directly measured to be 375–400°C with a temperature probe. The apparent shear rate ($\dot{\gamma}_{ap}$) in the extruder die was estimated to be 15 s^{-1} by eq. (2):[39]

$$\dot{\gamma}_{ap} = \frac{4Q}{\pi R^3} \quad (2)$$

where Q is the volumetric flow rate through a single die hole and R is the radius of an individual die. We recorded the extruder torque to determine the effects of the POSS concentration on processing by monitoring the torque output of the extruder after each composite system had reached steady state.

The PPSU resin was dried in a convection oven at 150°C overnight before blending. A master batch containing 10 wt % POSS was prepared by extrusion and further diluted by extrusion with neat PPSU resin to create PPSU/POSS nanocomposites containing Dp-POSS and Tsp-POSS at 0.5, 1, 2.5, 5, 7.5, and 10 wt % POSS. Specimens for tensile testing were injection-molded with a Mini-Jector model #55-1SOL by Miniature Plastic Molding (Solon, OH). Ten tensile bars for each sample were molded according to ASTM D 638 specifications for type 1 tensile bars. During molding, the temperatures of the barrel (366°C), die (368°C), and mold (104°C) were held constant, whereas the mold pressure was adjusted between 990 and 1500 psi to produce test specimens of appropriate dimensions. Once the correct mold pressure was determined for each POSS/PPSU composition, subsequent sample specimens had dimensions within the acceptable tolerance level.

GPC

GPC was used to determine the number-average molecular weight (M_n) and weight-average molecular weight (M_w) with a Waters GPC system (Milford, MA; dimethylformamide eluent, Waters 2420 ELS detector, and 1525 binary high performance liquid chromatography (HPLC) pump, Styragel HR 3 dimethylformamide and HR 4 columns). The system was calibrated with Shodex polystyrene standards from Waters, with molecular weights of 1060, 13,900, 55,100, and 197,000. Data was analyzed with Breeze version 3.3 software (Milford, MA, USA). Relative molecular weights based on polystyrene standards are reported.

Thermal characterization

The glass-transition temperature (T_g) was measured with a differential scanning calorimeter (model Q200 DSC, TA Instruments, New Castle, DE). Samples were heated in nitrogen at a flow rate of 50 mL/min from room temperature to 350°C at a heating rate of 10°C/min to remove the thermal history of the samples. The samples were then cooled and reheated to 350°C at a rate of 10°C/min, and T_g was recorded from the second heating scan as the temperature on the curve halfway between the tangent lines drawn above and below the transition region.

The thermal degradation behavior of the PPSU and POSS/PPSU composites in air at a flow rate of

40 mL/min was studied with a thermogravimetric analyzer (model Pyris 6, PerkinElmer, Waltham, MA). The samples were heated from room temperature to 850°C at a rate of 20°C/min. We defined the thermal degradation behavior of the blends by drawing a line tangent to the inflection point of the degradation curve obtained by TGA. The point where the tangent line crossed the line of 100% weight was the onset, and the point where the tangent line crossed the final steady (char) line was the end. TGA evaluations of the neat POSS materials were conducted on a TA Instruments Q500 at a heating rate of 10°C/min to a maximum temperature of 700°C in air. To ensure purity and remove any traces of solvent, the POSS samples were dried *in vacuo* at 60°C for a period of 8 h before TGA.

Optical microscopy

The dispersion and aggregation behavior of the POSS/PPSU composites was analyzed by optical microscopy with a Keyence VHX-600 digital microscope (Osaka, Japan) with an attached Keyence VH-Z100R polarized lens system (resolution = 100–1000×). Imaging was performed at various levels of magnification in polarized and unpolarized light environments.

Capillary rheometry

An LCR7000 capillary rheometer by Dynisco Instruments (Franklin, MA) was used to measure the apparent viscosity (η_{ap}) as a function of the shear rate at 380°C. The capillary bore had a radius (R) of 0.020″ and a length (L) of 0.800″ with a 120° degree entry angle. η_{ap} is the ratio of the apparent shear stress (τ_{ap}) to $\dot{\gamma}_{ap}$. With the dimensions of the capillary bore, the volumetric flow rate of the material through the capillary (Q) and the pressure differential across the capillary (ΔP), η_{ap} was calculated by eq. (3):

$$\eta_{ap} = \frac{\tau_{ap}}{\dot{\gamma}_{ap}} = \frac{\pi \Delta P R^4}{8QL} \quad (3)$$

Specified shear rates of 25, 100, 500, 1500, and 3500 s^{-1} were used for the viscosity measurements.

Tensile testing

The tensile properties (modulus of elasticity, tensile strength, percentage elongation at yield, and percentage elongation at break) were measured according to ASTM D 638 with a universal testing machine by MTS (Eden Prairie, MN). PPSU is a hygroscopic material, and samples were conditioned before testing by placement in a convection oven at 140°C for a minimum of 5 h to remove any moisture and then cooling to room temperature in a desiccation chamber before testing. Testing took place in a temperature- (27°C) and humidity- (40–45%) controlled room. Ten specimens for each sample were tested, and the speed of testing was set at 2 in./min.

TABLE I
Molecular Weights of the PPSU and POSS/PPSU Composites as Measured by GPC

	$M_w \times 10^{-4}$	$M_n \times 10^{-4}$	M_w/M_n
Neat PPSU	9.21	2.29	4.02
0.5% Tsp-POSS	8.65 (−6.08)	2.21 (−3.49)	3.91
1.0% Tsp-POSS	9.12 (−0.98)	2.43 (6.11)	3.75
2.5% Tsp-POSS	9.72 (−5.54)	1.99 (−13.10)	4.88
5.0% Tsp-POSS	9.68 (−5.10)	2.54 (10.92)	3.81
7.5% Tsp-POSS	9.74 (5.75)	2.32 (1.31)	4.20
10.0% Tsp-POSS	9.42 (2.28)	2.14 (−6.55)	4.40
0.5% Dp-POSS	9.83 (6.73)	2.26 (−1.31)	4.35
1.0% Dp-POSS	9.81 (6.51)	2.10 (−8.30)	4.67
2.5% Dp-POSS	9.80 (6.41)	2.20 (−3.93)	4.45
5.0% Dp-POSS	10.00 (8.58)	2.12 (−7.42)	4.72
7.5% Dp-POSS	9.68 (−5.10)	2.06 (−10.04)	4.70
10.0% Dp-POSS	8.67 (−5.86)	1.92 (−16.16)	4.52

The values in parentheses represent the percentage change in the molecular weight in relation to the neat PPSU.

RESULTS AND DISCUSSION

GPC

M_w, M_n, and the polydispersity index (PDI) for the blends determined by GPC are presented in Table I. The values in parenthesis and italics to the right of the measured molecular weights represent the percentage change of the POSS/PPSU composites' molecular weights relative to those of PPSU. The measured molecular weights for the blends are generally within 5 to 10% of the measured molecular weight for the neat PPSU, and the PDIs are generally within approximately 10% of that of the neat PPSU. The variations appeare to be randomly distributed (higher or lower than neat PPSU) and are attributed to experimental variation rather than any significant degradation or crosslinking of the polymer matrix on addition of POSS. The PDI shows a similar trend.

Thermal characterization

T_g and the thermal degradation behavior of the POSS/PPSU composites are shown in Table II. T_g of pure PPSU was observed at 222°C, and the T_g's of all of the Tsp-POSS and Dp-POSS composites were within 1% of that of pure PPSU. The data in Table II also indicate that the addition of Tsp-POSS or Dp-POSS up to 10 wt % did not affect the T_g behavior of PPSU. This type of behavior has been observed in

TABLE II
Glass-Transition and Thermal Degradation Behavior of the POSS, PPSU, and POSS/PPSU Composites

	T_g (°C)	Degradation onset (°C)	Degradation inflection (°C)	Degradation end (°C)	Residual weight (%)
Neat Dp-POSS	—	342	—	—	42.0
Neat Tsp-POSS	—	231	—	—	45.2
Neat PPSU	222	564	594	623	48.0
2.5% Tsp-POSS	222	570	600	633	47.8
5.0% Tsp-POSS	221	574	609	636	47.8
7.5% Tsp-POSS	222	576	610	638	47.8
10.0% Tsp-POSS	222	582	615	641	49.9
2.5% Dp-POSS	222	562	596	632	47.1
5.0% Dp-POSS	220	571	607	636	48.0
7.5% Dp-POSS	221	567	599	629	47.4
10.0% Dp-POSS	221	566	600	631	47.5

DSC was conducted in nitrogen, and TGA was conducted in air.

other POSS/polymer melt-blended systems and has generally been attributed to limited interaction between the polymer and the dispersed POSS molecules.[18,27,40,41] In cases where strong interchain interactions are observed between POSS crystallites and the polymer chain, significant increases in T_g may be observed.[40] Thus, it was indicated that in our system, there was limited molecular interaction between the POSS molecules and the PPSU chains. DSC evaluation of the neat POSS samples revealed a first-order transition for Tsp-POSS at 236°C. It has been reported that trisilanol POSS molecules undergo condensation reactions that result in a mixture of products when they are heated above 220°C.[42] Thus, we termed this a *solid-to-liquid transition* rather than a single crystalline melting point. Dp-POSS exhibited two first-order transitions, at 320 and 366°C. The lower temperature transition may be attributed to a crystalline form transition and the higher temperature transition is considered to be the melting point.[22,40]

TGA of PPSU and POSS/PPSU showed one-step degradation profiles. The neat POSS samples, however, showed multistep degradation profiles (Fig. 3). Although the onset temperature of degradation for the neat POSS samples was substantially lower than that of PPSU (231°C for Tsp-POSS, 342°C for Dp-POSS, and 564°C for PPSU), significant degradation (>5%) did not occur until around 400°C. The initial mass loss in the Tsp-POSS sample was attributed to the condensation and rearrangement reactions that occurred around 230°C. In the PPSU/POSS composites, however, these lower temperature losses were not observed (most likely because the concentrations of POSS were low), and the POSS molecules did not appear to accelerate the degradation of PPSU. In fact, although the degradation profiles of the Dp-POSS/PPSU blends were similar to that of neat PPSU, the composites containing Tsp-POSS exhibited a gradual increase in temperatures associated with the degradation onset, inflection, and end, which was proportional to the concentration of Tsp-POSS. At 10 wt % Tsp-POSS in PPSU, the onset of degradation increased by 18°C, the inflection point increased by 21°C, and the end increased by 18°C. On the basis of these results, the thermal stability of PPSU was increased by approximately 2–3% with the 10 wt % addition of Tsp-POSS. The residual weight of the Dp-POSS nanocomposites at the end of the heating ramp remained constant relative to PPSU but a small increase of 2 wt % was observed in the residual weight of the 10 wt % Tsp-POSS composite. The increase in the residual weight of the 10 wt % Tsp-POSS composite coincides with the observed increase in degradation temperatures associated with this composite. The thermal degradation behavior presented in Table II agreed with measurements made by GPC and further indicated that the addition of POSS to PPSU did not induce degradation, crosslinking, or unwanted chemical reactions. Analysis of the thermal behavior of Tsp-POSS composites suggested that the addition of Tsp-POSS actually improved the thermal degradation behavior of PPSU. POSS has been shown to improve flame retardancy in polymeric materials through formation

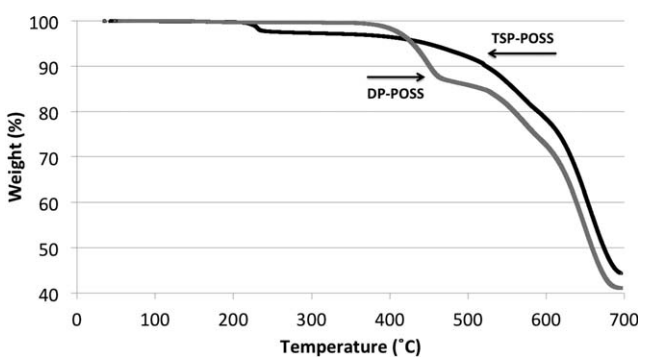

Figure 3 TGA degradation profiles of Tsp-POSS and Dp-POSS in air.

of a char layer that serves as an oxygen barrier and inhibits degradation,[11,43] and this may explain the enhanced stability exhibited in the Tsp-POSS/PPSU system.

Solubility parameter estimation

The solubility parameter of PPSU was calculated to be 10.1 $(cal/cm^3)^{1/2}$ using the second virial coefficient (A_2) of PPSU in 1-methyl-2-pyrollidinone (NMP) measured by static light scattering[44] and eqs. (4) and (5):

$$\chi_0 = 0.5 - \rho_j^2 V_i A_2 \tag{4}$$

where χ_0 is the Flory–Huggins interaction parameter between PPSU and NMP as the concentration approaches zero, ρ_j is the density of the polymer, and V_i is the solvent molar volume. NMP was a good solvent for PPSU, and χ_0 was assumed to be independent of concentration.[45] The entropic term of the Flory–Huggins interaction parameter is neglected; this yields the following relation:

$$\chi_0 = \left(\frac{V_i}{RT}\right)(\delta_i - \delta_j)^2 \tag{5}$$

where R is the ideal gas constant, T is temperature, δ_i is the solvent solubility parameter, and δ_j is the solubility parameter of the polymer.[35] Using the Hoy method,[36] we calculated the solubility parameters of Dp-POSS and Tsp-POSS to be 10.5 and 12.3 $(cal/cm^3)^{1/2}$, respectively. The solubility parameter calculated for the predominant form of the condensed Tsp-POSS formed on heating[42] was calculated to be 12.0. On the basis of the difference between the calculated POSS solubility parameters and that of PPSU, Dp-POSS ($\Delta\delta = 0.4$) was expected to have a lower ΔH_m with PPSU than Tsp-POSS ($\Delta\delta = 2.2$) and, thus, a higher solubility in the PPSU matrix.[46]

Composite processing and rheology

The torque on the extruder screws is directly proportional to the viscosity of the material being processed. Monitoring extruder torque during compounding is an effective method for quantifying the effects of POSS on material processing and nanocomposite viscosity. The extruder torque is presented as a function of the POSS concentration in Figure 4. For both the Dp-POSS and Tsp-POSS nanocomposite systems, substantial torque reductions (and, thus, improvements in the material processing) were observed.

The Tsp-POSS composites showed a linear relationship between the torque reduction and Tsp-POSS concentration. An approximately 3% reduction in torque was observed for every 1 wt % increase in the Tsp-POSS concentration. The Dp-POSS composites, on the other hand, exhibited a nonlinear response, with strong initial reductions in the extruder torque at low concentrations, which leveled off at concentrations of Dp-POSS above 5 wt %.

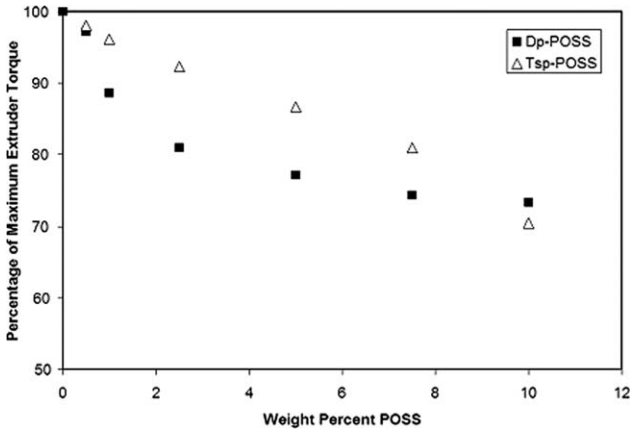

Figure 4 Reduction in the extruder torque during the melt blending of POSS and PPSU.

This behavior was contrary to what is typically observed for rigid particulate-filled systems, where the viscosity increases with loading level. It appeared to be related to the POSS melt transitions. The observed melting temperatures during extrusion ranged from 375 to 400°C. On the basis of our DSC results and the reported melting ranges for these POSS molecules,[47] we assumed that both Tsp-POSS and Dp-POSS were in the liquid state during extrusion. Under these conditions, POSS acted as a viscosity modifier and effectively promoted flow.

Reductions in the mold pressure, or hold pressure, provided a second indication of process enhancement. The mold pressure was increased to a maximum value to obtain optimum part densification without flashing. Less viscous polymer melts have a greater propensity to flash than those with higher viscosities. Therefore, the observation of the mold pressure during injection molding provides information about the melt viscosity. The mold pressures required to produce tensile test specimens of appropriate dimensions without flashing as a function of the POSS concentration are shown in Figure 5. A similar trend to that observed during extrusion was observed during the injection-molding process. For both types of POSS, the mold pressure was reduced as a function of increasing POSS concentration; this indicated enhanced processability. A linear relationship between the pressure and Tsp-POSS concentration was observed, whereas Dp-POSS exhibited the greatest percentage reductions at low concentrations, which leveled off at higher concentrations.

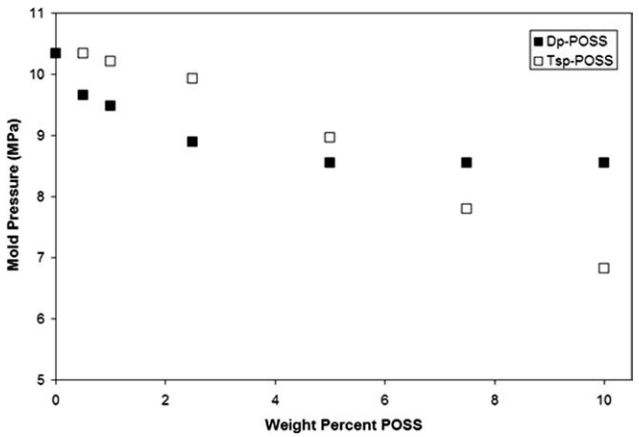

Figure 5 Reduction in the mold pressure during the injection molding of the test specimens.

The molded tensile bars of PPSU were highly transparent with an amber color. Upon addition of only 0.5 wt % Dp-POSS or Tsp-POSS, the specimens became cloudy. The further addition of Dp-POSS or Tsp-POSS caused the specimens to become opaque; this indicated agglomeration of the POSS nanostructured chemicals. Agglomeration and dispersion in molded test specimens were further investigated with optical microscopy. Representative optical micrographs of the molded POSS/PPSU test specimens containing 5% POSS are shown in Figure 6. Tsp-POSS/PPSU composites showed relatively homogeneous surfaces at all loading levels tested [Fig. 6(C,D)]. Dp-POSS composite surfaces showed aggregates on the order of micrometers at concentrations above 1%. The size of the aggregates increased with increasing POSS concentration. The aggregates appeared isolated within a homogeneous matrix, and for the 5 wt % Dp-POSS sample, their dimensions ranged from a few micrometers to greater than 100 μm [Fig. 6(A,B)]. It was not possible at this resolution to observe POSS crystallite structures in the polarized optical microscopy images.

Capillary rheometry data for Tsp-POSS/PPSU and Dp-POSS/PPSU blends as a function of POSS concentration are shown in Figures 7 and 8. All of the blends and neat PPSU exhibited shear thinning behavior, and the addition of POSS generally decreased η_{ap} of the blend. As observed in the extruder torque and mold pressure studies, η_{ap} decreased regularly with increasing Tsp-POSS concentration. Continuous reductions in η_{ap} were observed over the entire shear regime for concentrations up to 10 wt % Tsp-POSS (Fig. 7). On the other hand, in the Dp-POSS/PPSU composite systems, η_{ap} was strongly

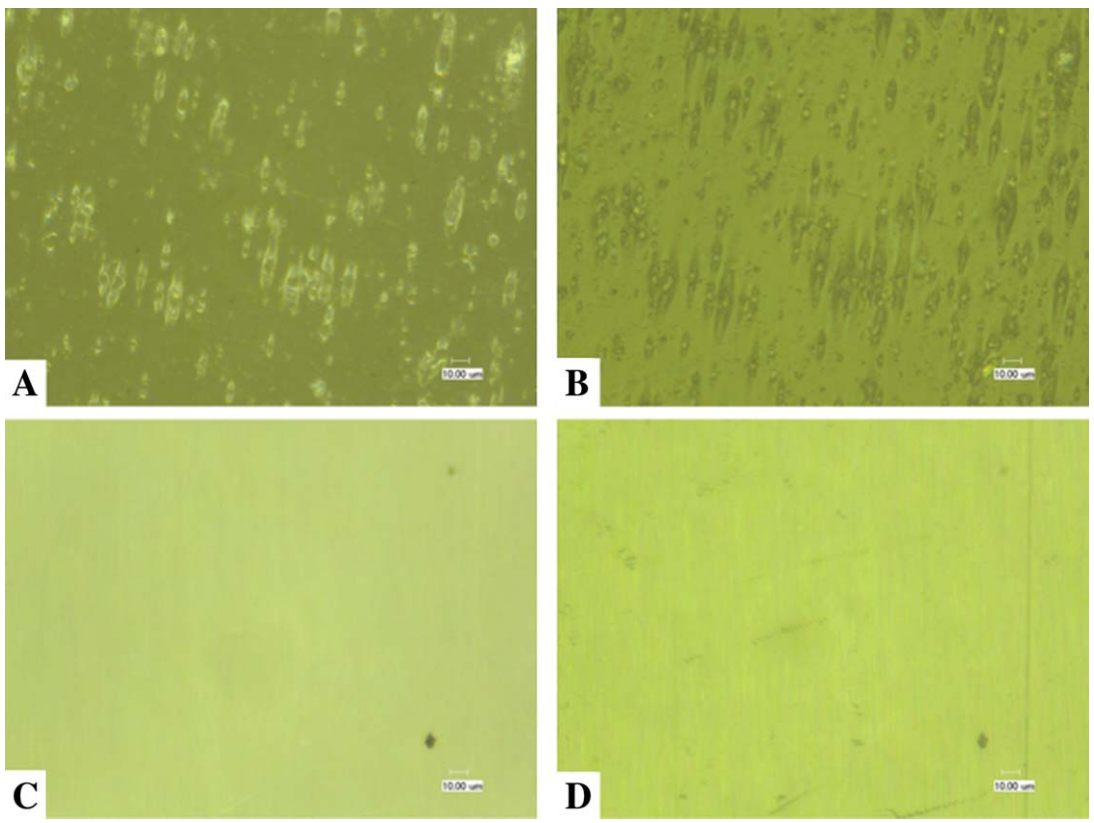

Figure 6 Optical micrographs of selected 5 wt % POSS/PPSU composites at 1000× magnification: (A) unpolarized Dp-POSS, (B) polarized Dp-POSS, (C) unpolarized TSP-POSS, and (D) polarized TSP-POSS. [Color figure can be viewed in the online issue, which is available at wileyonlinelibrary.com.]

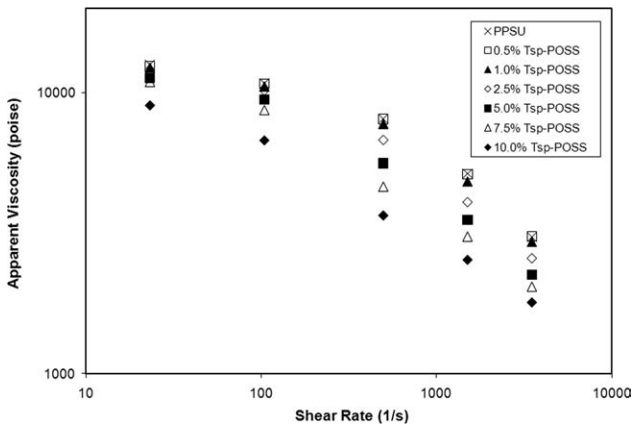

Figure 7 Log–log plot of η_{ap} as a function of the POSS concentration as measured by the capillary rheometry of the Tsp-POSS composites.

reduced at low POSS concentrations (Fig. 8). Nanocomposites containing 2.5 wt % Dp-POSS displayed the greatest viscosity reductions over the entire shear regime. At loadings higher than 2.5 wt % Dp-POSS, η_{ap} increased, particularly at shear rates ranging from 25 to 1500 s^{-1}. At the highest shear rate, the greatest overall viscosity reductions were observed for 2.5, 5, and 10 wt % composites. This behavior was similar to the processing behavior observed in both material compounding and injection-molding studies.

Substantial linear decreases in the extruder torque, mold pressure, and η_{ap} were observed for Tsp-POSS systems. Tsp-POSS has a considerably lower viscosity (estimated as 2 Pa s)[48] than PPSU. The application of a mixing rule can be used to predict the viscosity (η) of a phase-separated polymer mixture. For mixtures containing a high volume fraction of the more viscous component, the additivity model is representative:[36]

$$\eta_{composite} = \phi_1\eta_1 + \phi_2\eta_2 \quad (6)$$

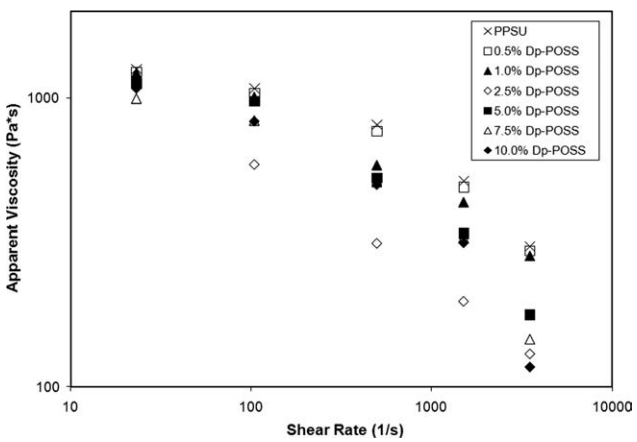

Figure 8 Log–log plot of η_{ap} as a function of the POSS concentration as measured by the capillary rheometry of the Dp-POSS composites.

where ϕ is the volume fraction and the subscripts refer to the components of the mixture. However, when there is poor adhesion between the phases, interfacial slippage can occur. This results in negative deviation from the additivity model, and strong reductions in viscosity can occur at very low volume fractions of the less viscous component.[49] The difference in the solubility parameters between Tsp-POSS and PPSU ($\Delta\delta = 1.3$) suggested there may have been poor adhesion between phases. In Figure 9, the viscosity predicted by the additivity rule and the measured η_{ap} (at a shear rate of 25 s^{-1}) for the Tsp-POSS/PPSU composites are compared as a function of the Tsp-POSS volume fraction. It was apparent that negative deviation from the additivity model occurs in this system, and Tsp-POSS has a strong internal lubricating effect on PPSU. In addition, evidence from tensile testing, which is discussed later, implied that Tsp-POSS underwent surface-phase segregation, which further improved the processing by reducing the friction between the composite melt and the steel components in the extruder or mold cavity.

The rheological behavior of the Dp-POSS/PPSU composites was significantly more complicated than that of the Tsp-POSS/PPSU composites. Because Dp-POSS has a melting range that is similar to the processing temperatures of PPSU, it is possible that Dp-POSS was not completely melted in the time frame of the experiments. On the basis of the observed agglomerates in optical micrographs, it is likely that a certain portion of the melted Dp-POSS entered the amorphous PPSU matrix, as would be expected by the similarity in their solubility parameters ($\Delta\delta = 0.4$). However, the solid Dp-POSS resided in a separate phase and was not incorporated into the PPSU matrix. After the solubility limit of Dp-POSS in PPSU was reached, the remaining

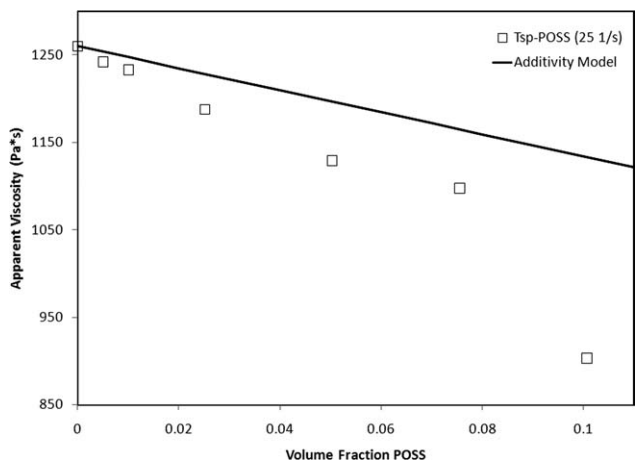

Figure 9 Viscosity predicted by the additive rule and η_{ap} (as measured by capillary rheometry at a shear rate of 25 s^{-1}) versus the Tsp-POSS volume fraction for the Tsp-POSS/PPSU composites.

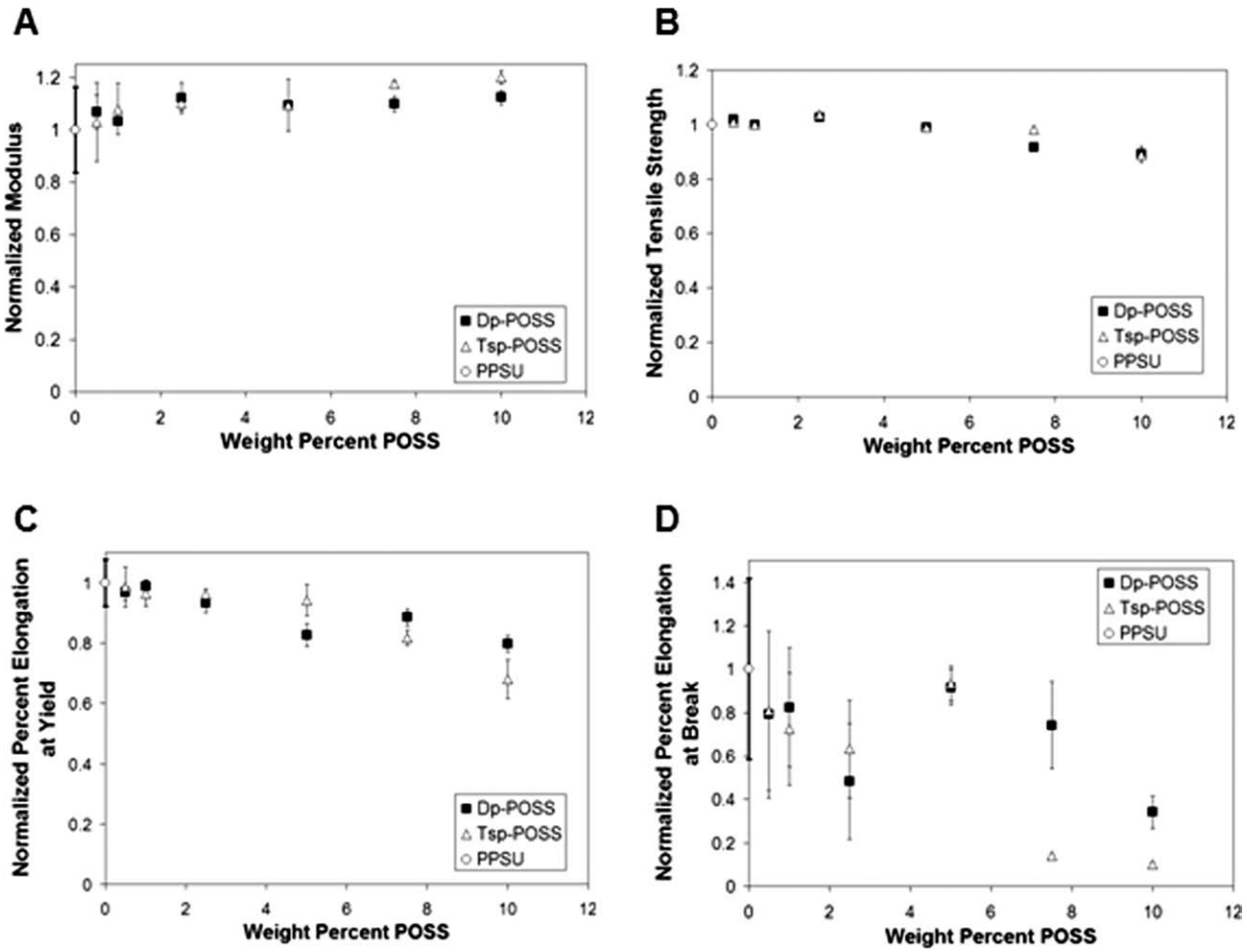

Figure 10 Tensile properties of the POSS/PPSU composites: (A) normalized modulus of elasticity, (B) normalized tensile strength, (C) normalized percentage elongation at yield, and (D) normalized percentage elongation at break.

Dp-POSS domains resided in the matrix as droplets containing a mixture of liquid and solid Dp-POSS. Three factors were identified that possibly contributed to the observed behavior of Dp-POSS. The strong initial reductions in the viscosity of the Dp-POSS composite systems at low concentrations may have been due to the nanoparticle effect previously described. As the concentration of Dp-POSS was further increased, partially melted Dp-POSS molecules acted as a lubricant; this served to improve the processing and reduce the viscosity. At higher concentrations, solid aggregates of Dp-POSS served to increase the viscosity, as observed in capillary rheometry.

Tensile properties

The tensile properties of the composite materials are presented in Figure 10 and Table III. The modulus of elasticity [Fig. 10(A)] and tensile strength [Fig. 10(B)] associated with the Dp-POSS and Tsp-POSS composite systems were within the standard deviation for the measured PPSU control at low concentrations. As the concentration of POSS was increased, a slight increase in the modulus accompanied by a small reduction in the tensile strength was observed in both systems. Although the Dp-POSS and Tsp-POSS composite materials retained their high modulus and tensile strength, a loss in ductility was observed at higher loadings of Dp-POSS and Tsp-POSS [Figs. 10(C,D)]. The percentage elongation at yield was maintained at low additions, but a decrease was observed at loading levels of 5 wt % and greater. Although all samples exhibited a high degree of variation in the percentage elongation at break measurement (PPSU standard exhibited variation = ±40%), a general decrease in the measured values was observed as a function of the POSS loading level. At higher concentrations (>5 wt %), the composite materials exhibited behavior similar to those observed with traditional fillers, whereas at lower concentrations (<5 wt %), the tensile properties of the composite systems were relatively maintained. These tensile results paralleled the observations made by Shiraldi et al.[18] in their work with Tsp-POSS/polycarbonate systems.

TABLE III
POSS/PPSU Composite Tensile Properties

	Tensile modulus (GPa)	Tensile strength (kpsi)	Elongation (%)
PPSU	0.798 (0.13)	10.9 (0.072)	120 (50)
0.5% Tsp-POSS	0.852 (0.052)	11.1 (0.046)	95 (46)
1.0% Tsp-POSS	0.824 (0.042)	10.9 (0.092)	99 (33)
2.5% Tsp-POSS	0.895 (0.047)	11.2 (0.063)	58 (32)
5.0% Tsp-POSS	0.873 (0.079)	10.8 (0.067)	112 (9.6)
7.5% Tsp-POSS	0.877 (0.024)	10.0 (0.056)	89 (24)
10.0% Tsp-POSS	0.897 (0.021)	9.73 (0.031)	42 (9.1)
0.5% Dp-POSS	0.822 (0.12)	11.0 (0.065)	97 (44)
1.0% Dp-POSS	0.862 (0.079)	10.9 (0.061)	87 (31)
2.5% Dp-POSS	0.880 (0.023)	11.3 (0.032)	76 (27)
5.0% Dp-POSS	0.873 (0.079)	10.8 (0.067)	112 (9.6)
7.5% Dp-POSS	0.939 (0.0094)	10.6 (0.078)	17 (0.57)
10.0% Dp-POSS	0.959 (0.021)	9.71 (0.324)	12 (1.1)

The values in parentheses represent one standard deviation.

The complex fracture behavior that occurred during elongation provided valuable insight into the surface segregation behavior and interfacial adhesion in the POSS/PPSU systems investigated (Fig. 11). The Dp-POSS composites exhibited necking until fracture for all compositions. However, in the 10.0 wt % Dp-POSS composite, the surface crazed, and then, the core region necked until fracture [Fig. 11(C)]. The Tsp-POSS composites ceased to display necking at concentrations of 7.5 and 10.0 wt % Tsp-POSS [Fig. 11(A)]. The skin of the test Tsp-POSS specimens fractured first; this was followed by a slight necking of the core region and then complete fracture. Strong delamination was observed between the skin and the core region. The occurrence of a surface fracture or crazing before a core fracture implied that the surfaces of the composite specimens were more brittle and enriched with POSS. The presence of delamination in the Tsp-POSS composite and the absence of delamination in the Dp-POSS composite indicated that Dp-POSS interacted more strongly with the PPSU matrix than Tsp-POSS, as predicted by the difference in the solubility parameters between these two materials and PPSU. In fact, the delamination and homogeneous surface morphology of the Tsp-POSS fracture surfaces together provided evidence that a film with a high Tsp-POSS concentration formed on the surface of the articles produced during injection molding.

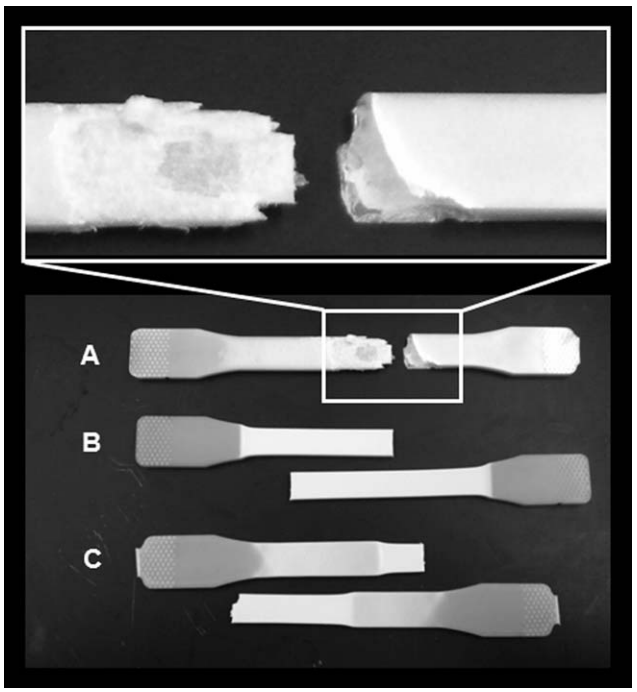

Figure 11 Selected photographs of the fractured tensile test specimens: (A) 10.0 wt % Tsp-POSS, (B) 7.5 wt % Dp-POSS, and (C) 10.0 wt % Dp-POSS.

CONCLUSIONS

Substantial material processing enhancement was observed in POSS/PPSU composites without detrimental effects on the thermal stability, T_g, or molecular weight of the PPSU resin for both types of POSS additive. The consistent, monotonic process improvements observed in the Tsp-POSS composite systems were attributed to internal lubrication resulting from the weak interfacial interactions between phases and the surface segregation of Tsp-POSS, which lubricated the exterior of the composite melt and reduced friction during processing. The rheological behavior of the Dp-POSS composites was significantly more complex, as explained by the fact that Dp-POSS may have existed as a mixture of liquid and solid during the melt experiments. At low concentrations of Dp-POSS, significant improvements in the material processing of PPSU occurred. As the Dp-POSS concentration increased, the process enhancements diminished; however, typical behavior of microfillers was not observed. The exact mechanism for this behavior

remains unknown, but we speculate it to be a combination of the nanoparticle effect, internal lubrication by melted Dp-POSS, surface segregation, and the presence of large POSS aggregates.

Optical micrographs of the nanocomposite morphology and observations of the fracture mechanisms during tensile testing served to explain the complex behavior of the Dp-POSS and Tsp-POSS composite systems. Morphological images of the Dp-POSS composites at low concentrations ($\leq$1 wt % Dp-POSS) appeared homogeneous, and the tensile properties of these systems were maintained. Large micrometer-scale aggregates at higher concentrations caused the mechanical properties of this system to resemble a rigid particulate-filled material. The homogeneous morphology observed in the Tsp-POSS fracture surfaces systems combined with their observed delamination during fracture suggested that Tsp-POSS was enriched at the composite surface during processing.

Although solubility parameter matching can provide an indication of compatibility, it cannot be used as the sole predictor of rheology enhancement. Optical analysis of the composite systems showed them to be in a state of incompatibility, where only a small quantity of either Dp-POSS or Tsp-POSS was dissolved in the PPSU matrix. The incompatibility observed in the Dp-POSS composites may have arisen because of incomplete melting of the Dp-POSS crystals during blending, whereas the incompatibility observed in Tsp-POSS composite systems was a result of differences in the melt viscosities of Tsp-POSS and PPSU and surface segregation attributed to poor solubility in the PPSU matrix.

The versatile and highly adaptable nature of the hybrid organic–inorganic POSS structure provides the opportunity for rheology enhancement in a range of polymer systems. Multiple factors, including the melting temperature, polymer/POSS viscosity match, loading level, and chemical structure, must be considered in predicting the rheological performance. In addition, the propensity of POSS to undergo surface segregation provides the opportunity for surface modification when POSS is incorporated into a thermoplastic matrix.

The authors thank Hybrid Plastics for providing POSS materials and for useful discussions.

References

1. Lichtenhan, J. D. Comments Inorg Chem 1995, 17, 115.
2. Shockey, E. G.; Bolf, A. G.; Jones, P. F.; Schwab, J. J.; Chaffee, K. P.; Haddad, T. S.; Lichtenhan, J. D. Appl Organomet Chem 1999, 13, 311.
3. Lichtenhan, J. D.; Schwab, J. J.; Reinerth, W. A. Chem Innovation 2001, 31, 3.
4. Chen, G. X.; Shimizu, H. Polymer 2008, 49, 943.
5. Misra, R.; Alidedeoglu, A. H.; Jarrett, W. L.; Morgan, S. E. Polymer 2009, 50, 2906.
6. Wheeler, P. A.; Misra, R.; Cook, B.; Morgan, S. E.; Lichtenhan, J. D. J Appl Polym Sci 2008, 108, 2503.
7. Lee, A.; Lichtenhan, J. D. J Appl Polym Sci 1999, 73, 1993.
8. Lichtenhan, J. D.; Vu, N. Q.; Carter, J. A.; Gilman, J. W.; Feher, F. J. Macromolecules 1993, 26, 2141.
9. Mather, P. T.; Jeon, H. G.; Romo-Uribe, A.; Haddad, T. S.; Lichtenhan, J. D. Macromolecules 1999, 32, 1194.
10. Romo-Uribe, A.; Mather, P. T.; Haddad, T. S.; Lichtenhan, J. D. J Polym Sci Part B: Polym Phys 1998, 36, 1857.
11. Patel, R. R.; Mohanraj, R.; Pittman, C. U. J Polym Sci Part B: Polym Phys 2006, 44, 234.
12. Lee, A.; Lichtenhan, J. D. Macromolecules 1998, 31, 4970.
13. Turri, S.; Levi, M. Macromolecules 2005, 38, 5569.
14. Lee, A.; Xiao, J.; Feher, F. J. Macromolecules 2005, 38, 438.
15. Madbouly, S. A.; Otaigbe, J. U.; Nanda, A. K.; Wicks, D. A. Macromolecules 2007, 40, 4982.
16. Wu, J.; Haddad, T. S.; Mather, P. T. Macromolecules 2009, 42, 1142.
17. Fu, B. X.; Hsiao, B. S.; Pagola, S.; Stephens, P.; White, H.; Rafailovich, M.; Sokolov, J.; Mather, P. T.; Jeon, H. G.; Phillips, S.; Lichtenhan, J.; Schwab, J. Polymer 2001, 42, 599.
18. Zhao, Y.; Schiraldi, D. A. Polymer 2005, 46, 11640.
19. Fina, A.; Tabuani, D.; Frache, A.; Camino, G. Polymer 2005, 46, 7855.
20. Einstein, A. Ann Phys 1906, 19, 371.
21. Joshi, M.; Butola, B. S.; Simon, G.; Kukaleva, N. Macromolecules 2006, 39, 1839.
22. Kopesky, E. T.; Haddad, T. S.; Cohen, R. E.; McKinley, G. H. Macromolecules 2004, 37, 8992.
23. Zhou, Z.; Zhang, Y.; Zhang, Y.; Yin, N. J Polym Sci Part B: Polym Phys 2008, 46, 526.
24. Zhang, Q.; Archer, L. A. Langmuir 2002, 18, 10435.
25. Mackay, M. E.; Dao, T. T.; Tuteja, A.; Ho, D. L.; Van Horn, B.; Kim, H. C.; Hawker, C. J. Nat Mater 2003, 2, 762.
26. Misra, R.; Fu, B. X.; Morgan, S. E. J Polym Sci Part B: Polym Phys 2007, 45, 2441.
27. Misra, R.; Fu, B. X.; Plagge, A.; Morgan, S. E. J Polym Sci Part B: Polym Phys 2009, 47, 1088.
28. Tang, Y.; Lewin, M. Polym Adv Technol 2009, 20, 1.
29. Hosaka, N.; Otsuka, H.; Hino, M.; Takahara, A. Langmuir 2008, 24, 5766.
30. Paul, R.; Karabiyik, U.; Swift, M. C.; Hottle, J. R.; Esker, A. R. Langmuir 2008, 24, 5079.
31. Paul, R.; Karabiyik, U.; Swift, M. C.; Hottle, J. R.; Esker, A. R. Langmuir 2008, 24, 4676.
32. Koh, K.; Sugiyam, S.; Morinaga, T.; Ohno, K.; Tsuji, Y.; Fukuda, T.; Yamahiro, M.; Iijima, T.; Oikawa, H.; Watanabe, K.; Miyashita, T. Macromolecules 2005, 38, 1264.
33. Schiraldi, D. A.; Iyer, S. In Advances in Silicones and Silicone-Modified Materials; Clarson, S. J., Owen, M. J., Smith, S. D., Van Dyke, M. E., Eds.; ACS Symposium Series 1051; American Chemical Society: Washington, DC, 2010. DOI: 10.1021/bk-2010-1051.ch017, Chapter 17, pp 211 -226.
34. Liu, L.; Ming, T.; Liang, G.; Chen, L.; Zhang, L.; Mark, J. E. J Macromol Sci Pure Appl Chem 2007, 44, 659.
35. Barton, A. F. M. CRC Handbook of Polymer–Liquid Interaction Parameters and Solubility Parameters; CRC: Boca Raton, FL, 1990.
36. Robeson, L. M. Polymer Blends; Hanser: Munich, 2007.
37. Hoy, K. L. J Paint Technol 1970, 42, 76.
38. Solvay Advanced Polymers, LLC. Product Data RADEL R Polyphenylsulfone. http://solvayadvancedpolymers.com/static/wma/pdf/1/6/0/R5_1_500.pdf (accessed January 27, 2010).
39. Son, Y. Polymer 2007, 48, 632.
40. Li, S.; Simon, G.; Matisons, J. Polym Eng Sci 2010, 50, 991.

41. Kopesky, E.; Haddad, T.; McKinley, G.; Cohen, R. Polymer 2005, 46, 4743.
42. Feher, F. J.; Newman, D. A.; Walzer, J. F. J Am Chem Soc 1989, 111, 1741.
43. Lichtenhan, J. D.; Gilman, J. W. Preceramic Additives as Fire Retardants for Plastics; 2001. U.S. Patent Application; 13 p. May 28, 1997.
44. Jones, P. J.; Paslay, L. C.; Morgan, S. E. Polymer 2010, 48, 738.
45. Flory, P. J. Principles of Polymer Chemistry; Cornell University Press: Ithaca, NY, 1953.
46. Coleman, M. M.; Graf, J. F.; Painter, P. C. Specific Interactions and the Miscibility of Polymer Blends; Technomic: Lancaster, PA, 1991.
47. Hybrid Plastics, Inc. Material Safety Data Sheet for Dodecaphenyl POSS MS0802 http://hybridplastics.com/products/bulk.htm (accessed March 8, 2010).
48. Hybrid Plastics, Inc. Personal communication.
49. Utraki, L. A.; Kamal, M. R. In Polymer Blends Handbook; Utraki, L. E., Ed.; Kluwer: Dordrecht, The Netherlands, 2002; Vol. 1.